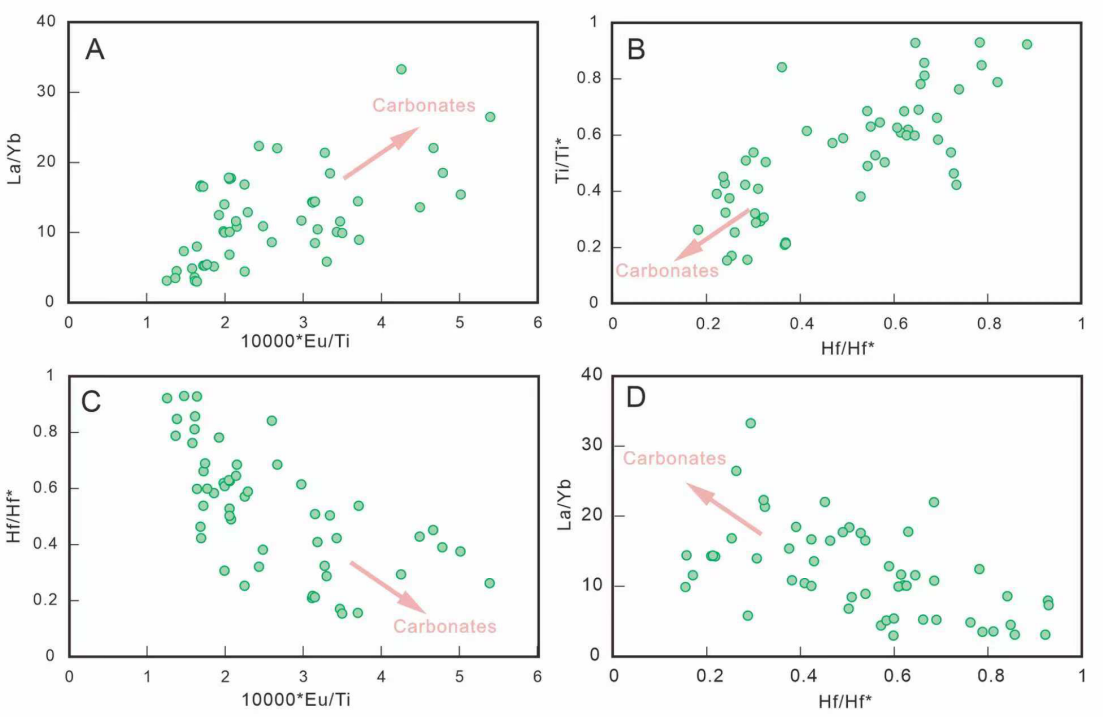

Extended Data Fig. 1 Variations of (A) La/Yb versus 10000*Eu/Ti, (B) Ti/Ti* versus Hf/Hf*, (C) Hf/Hf* versus 10000*Eu/Ti, and (D) La/Yb versus Hf/Hf* for the studied Neoarchean basalts. Elemental anomalies are calculated as follows: $Ti/Ti^* = Ti_N/(Sm_N^{-0.055} \times Nd_N^{0.333} \times Gd_N^{0.722})$, $Hf/Hf^* = Hf_N/(Sm_N \times Nd_N)^{0.5}$, where the subscript N means normalized to the primitive mantle.

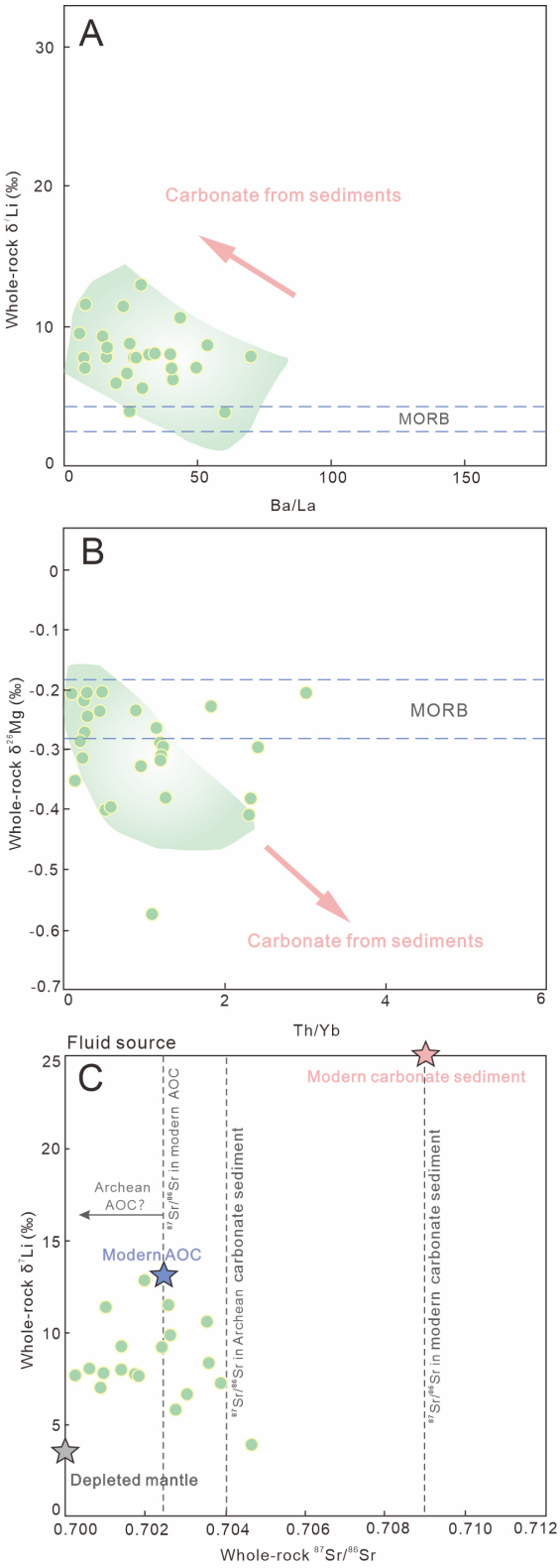

Extended Data Fig. 2 Isotopic and elemental ratios constrain the origins of carbon and fluids. (A) Plots of δ^{7}Li versus Ba/La, (B) Plots of δ^{26}Mg versus Th/Yb and (C) Plots of δ^{7}Li versus $^{87}Sr/^{86}Sr$.

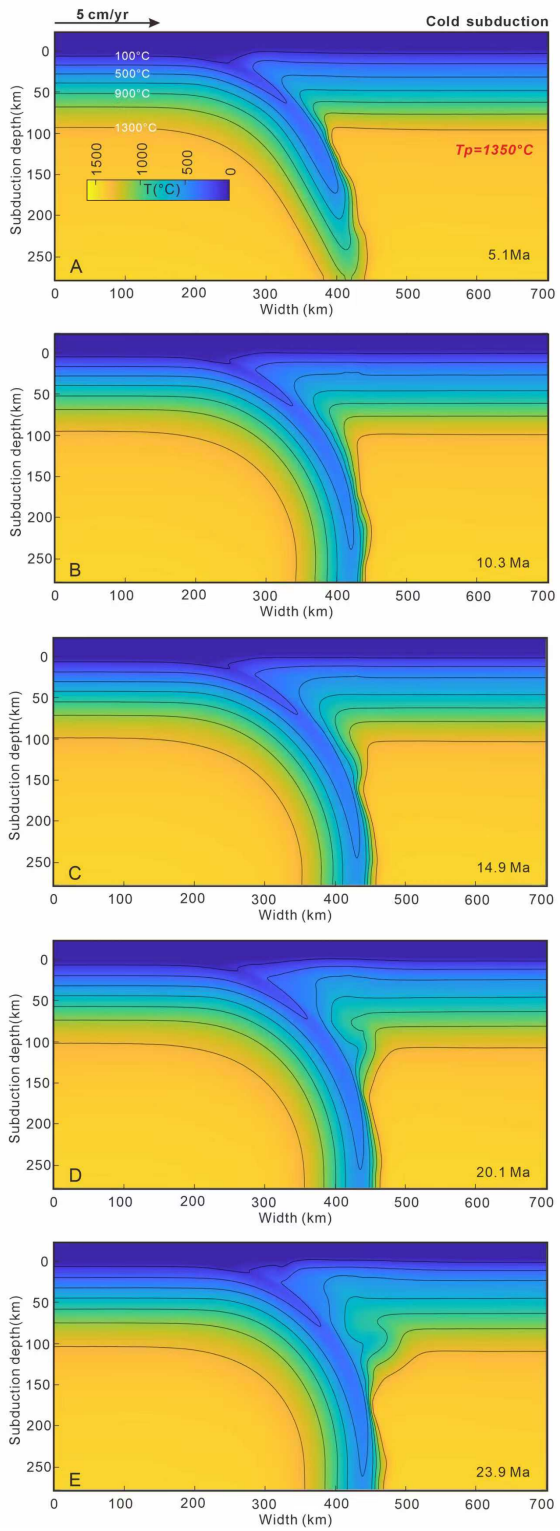

Extended Data Fig. 3 The temporal change in the subduction P-T field under the condition of Tp = 1350°C (modern).

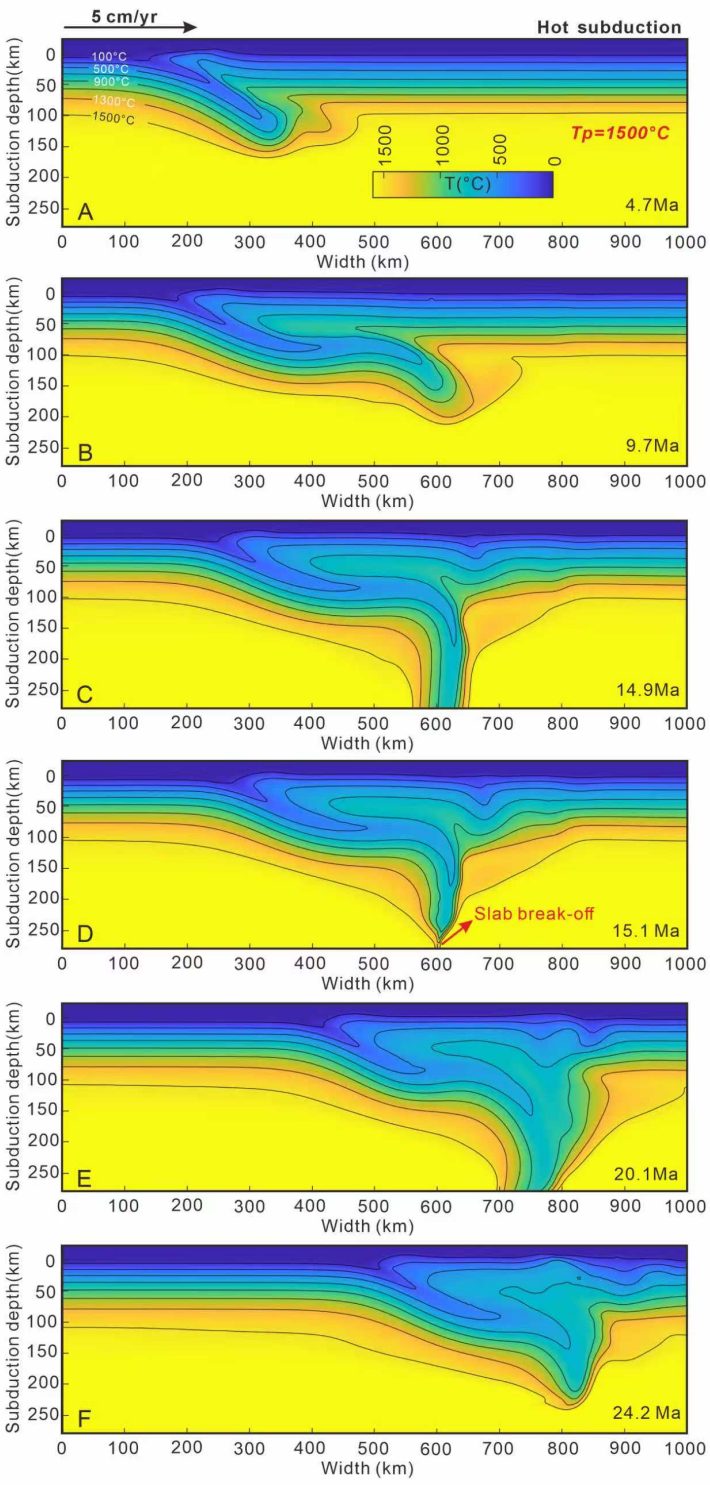

Extended Data Fig. 4 The temporal change in the subduction P-T field under the condition of Tp = 1500°C (Archean-Paleoproterozoic).

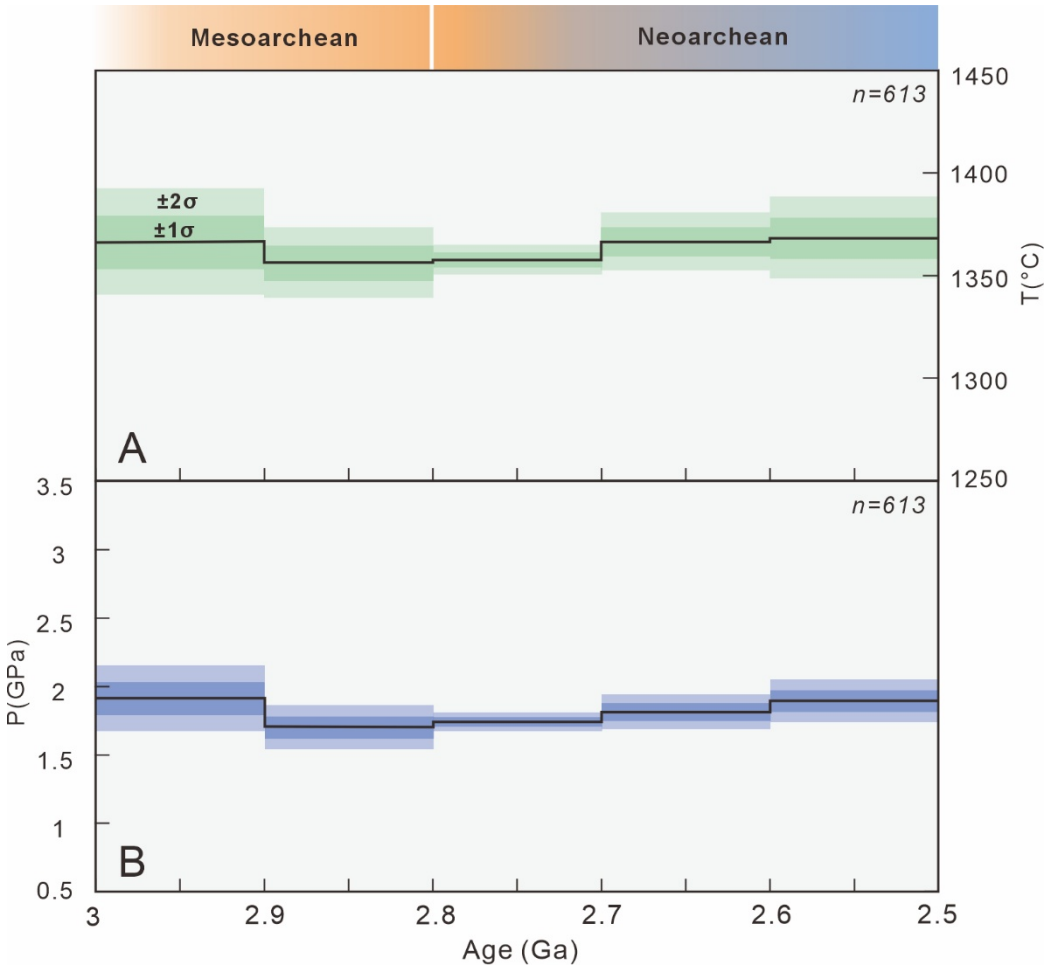

Extended Data Fig. 5 Formation Temperature and Pressure of Primary Arc Basalts over Time (3-2.5 Ga)

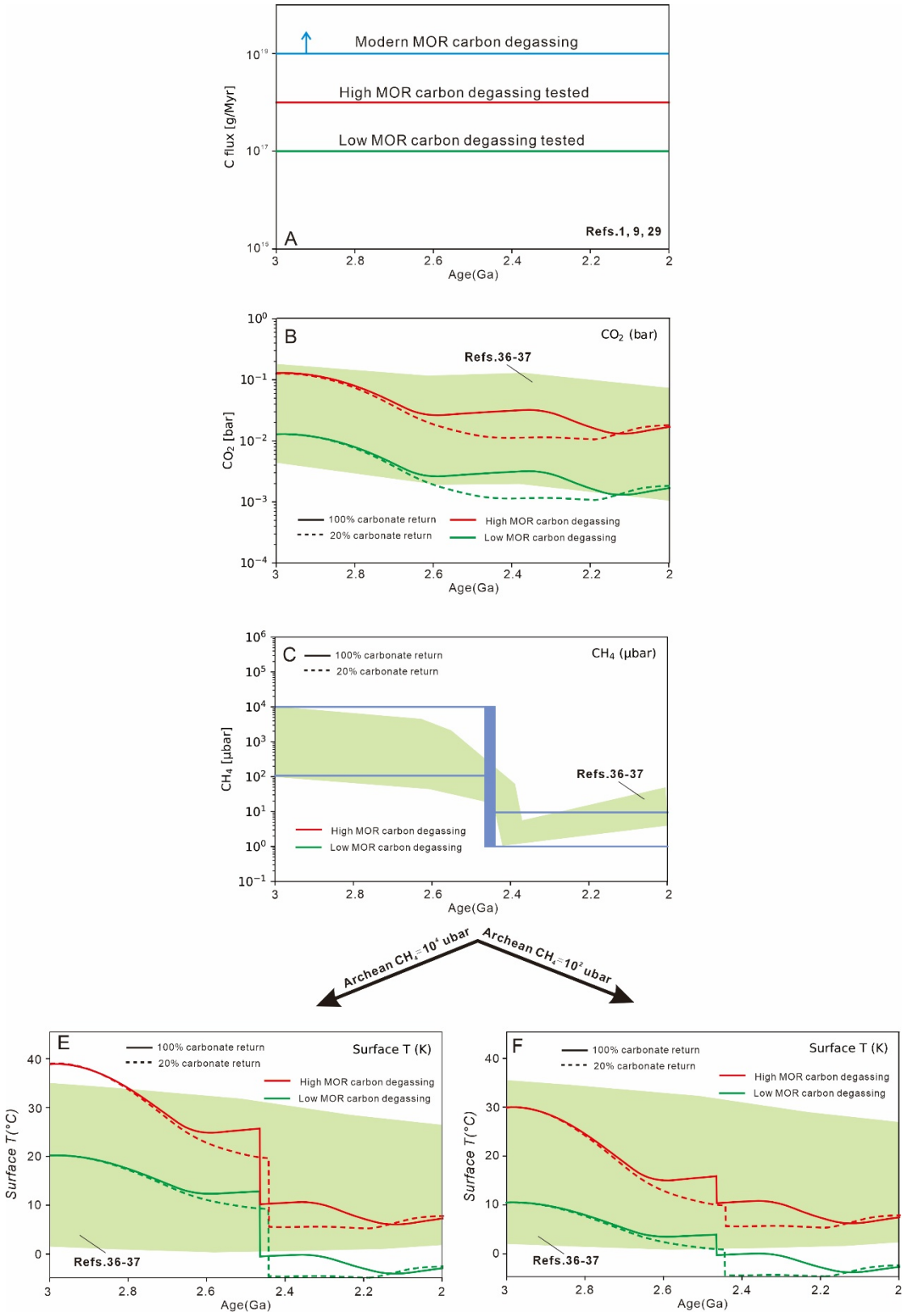

Extended Data Fig. 6 The tests of different initial MOR degassing and CH_4 concentrations in C-O box models collectively demonstrate the moderating effect of enhanced subduction biogeodynamic carbon cycling on temperature. The green background is a reference range in previous studies.

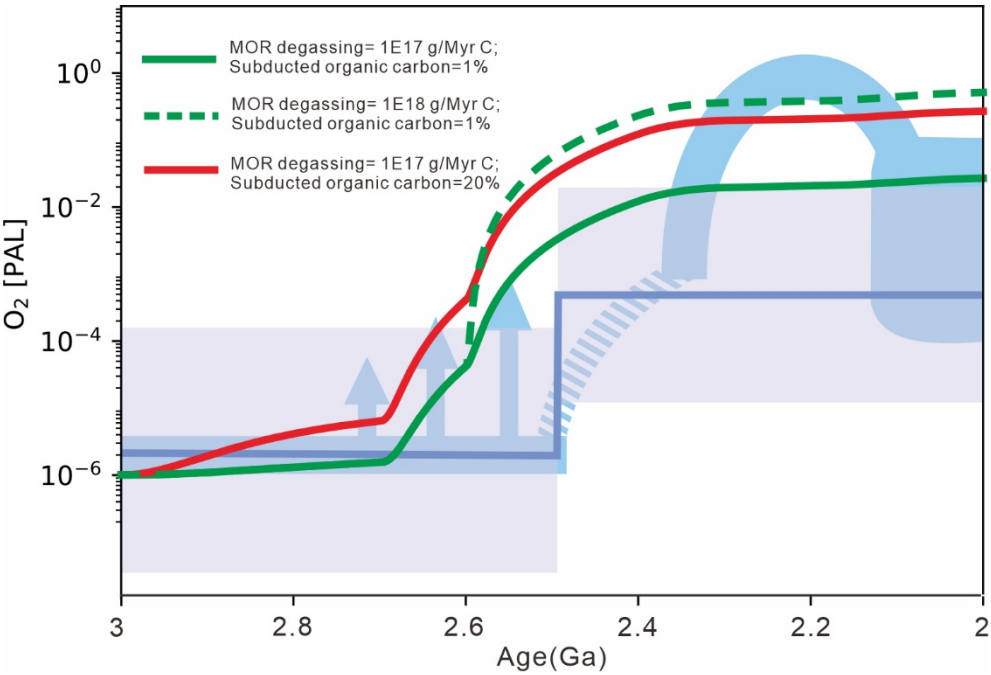

Extended Data Fig. 7 The tests of different initial MOR degassing and proportion of organic carbon in sediment in C-O box models collectively demonstrate the moderating effect of enhanced subduction biogeodynamic carbon cycling on O_2 levels.